Bone regenerative potential of the selective sphingosine 1-phosphate receptor modulator siponimod: *in vitro* characterisation using osteoblast and endothelial cells

Ziad Sartawi[1], Katie B. Ryan[1], Christian Waeber[1,2]

[1] *School of Pharmacy, University College Cork, Cork, Ireland*

[2] *Department of Pharmacology and Therapeutics, University College Cork, Cork, Ireland*

Corresponding author:

Christian Waeber

C.Waeber@ucc.ie

School of Pharmacy

University College Cork

College Rd

Cork T12 YN60

Ireland

Abstract

The repair of critical bone defects remains a significant therapeutic challenge. While the implantation of drug-eluting scaffolds is an option, a drug with the optimal pharmacological properties has not yet been identified. Agents acting at sphingosine 1-phosphate (S1P) receptors have been considered, but those investigated so far do not discriminate between the five known S1P receptors. This work was undertaken to investigate the potential of the specific $S1P_{1/5}$ modulator siponimod as a bone regenerative agent, by testing *in vitro* its effect on cell types critical to the bone regeneration process.

hFOB osteoblasts and HUVEC endothelial cells were treated with siponimod and other S1P receptor modulators and investigated for changes in intracellular cyclic AMP content, viability, proliferation, differentiation, attachment and cellular motility.

Siponimod showed no effect on the viability and proliferation of osteoblasts and endothelial cells, but increased osteoblast differentiation (as shown by increased alkaline phosphatase activity). Furthermore, siponimod significantly increased endothelial cell motility in scratch and transwell migration assays.

These effects on osteoblast differentiation and endothelial cell migration suggest that siponimod may be a potential agent for the stimulation of localised differentiation of osteoblasts in critical bone defects.

Keywords: Siponimod, Sphingosine 1-phosphate, $S1P_1$ Receptors, Osteoblasts, HUVEC

1. Introduction

The restoration of tissue function after damage, involves complex interactions between various cell types, local tissue matrix, and chemical mediators, in various combinations.

The creation of new vasculature via angiogenesis is essential for the regeneration of any tissue, and in the case of bones, regeneration also involves the recruitment of osteoblast and osteoclast precursors to the defect area, their differentiation into their mature phenotypes as well as interaction between the two cell types, with bone-forming osteoblasts stimulating the maturation of bone resorbing osteoclasts, which in turn stimulate osteoblast recruitment and maturation.

Sphingosine 1-phosphate (S1P) is a lipid mediator that modulates many biological processes, including calcium signalling, cell growth, differentiation, survival, motility and cytoskeleton organization (Spiegel and Milstien, 2000). It acts via 5 known G Protein-Coupled Receptors ($S1P_{1-5}$), which are widely expressed throughout the body (Hla, 2004). The role of S1P in promoting angiogenesis is well-established (Waeber, 2013). This, taken together with the pleiotropic effects of S1P on bone cells (Sartawi et al., 2017), suggests that modulating S1P signalling may promote bone repair. However, systemic administration of S1P agents did not improve fracture healing in a murine femoral defect (Heilmann et al., 2013), indicating that more localised approaches of delivering S1P and related analogues may be needed (Das et al., 2014b).

The pharmacological characterization of the various S1P-mediated responses, in bone and other tissues, has been hampered by the lack of well-characterized specific agents (Salomone and Waeber, 2011). S1P itself (with or without receptor antagonists), as well as the S1P receptor modulator fingolimod (aka FTY720 or Gilenya®) have been investigated in *in vitro* and *in vivo* models of bone repair (Sartawi et al., 2017), but these agents do not discriminate

between the 5 different receptor subtypes. Fingolimod, used clinically for the management of relapsing remitting multiple sclerosis, is a potent agonist at all S1P receptor subtypes except $S1P_2$ (Brinkmann et al., 2010). Its mechanism of action relies, at least in part, on the redistribution of lymphocytes to secondary lymphoid tissues following fingolimod-induced $S1P_1$ receptor internalization, resulting in their depletion from the peripheral blood and immunosuppression. Although fingolimod is relatively safe, activation of $S1P_3$ receptors by this agent may be associated with adverse effects (Cugati et al., 2014; DiMarco et al., 2014). Although the role of $S1P_3$ receptors in cardiac side effects may be unique to rodents (Gergely et al., 2012), these off-target effects led to the discovery and development of the $S1P_1$/$S1P_5$ selective agonist siponimod (aka BAF312, or Mayzent®) (Behrangi et al., 2019). In addition to its improved selectivity profile, siponimod is not a pro-drug (fingolimod must first be phosphorylated by sphingosine kinase 2) and has a shorter half-life that still allows once-daily oral dosing but enables rapid recovery of lymphocyte counts upon treatment cessation.

The effects of S1P and of fingolimod on cells relevant to bone repair have been extensively investigated (Sartawi et al., 2017), but far less is known on the effect of siponimod on these cells. The goal of these studies was therefore to test the effect of siponimod on the viability, proliferation, differentiation, and chemotactic behaviour of osteoblast and endothelial cells, with the aim of better understanding the potential of selective modulation of $S1P_1$ (or $S1P_5$) receptors via localised delivery to repair critical bone defects.

2. Material and methods

Siponimod and fingolimod were kindly gifted from Novartis. D-erythro-Sphingosine 1-phosphate was acquired from Enzo Life Sciences. Dulbecco's Modified Eagle's Medium/Nutrient Mixture F-12 Ham, foetal bovine serum (FBS), L-Glutamine, penicillin-streptomycin, Thiazolyl Blue Tetrazolium Bromide (MTT), dimethyl sulfoxide (DMSO),

neutral buffered formalin (NBF), Fast Blue BB and Naphthol AS-MX phosphate, Roche Bromodeoxyuridine cell proliferation kit were acquired from Sigma-Aldrich. Endothelial cells (HUVEC) and endothelial cell growth medium (ECGM) with associated supplements were acquired from PromoCell. Pierce™ PNPP Substrate Kit was acquired from Thermo Fisher Scientific. cAMP-Glo™ Max Assay was acquired from Promega. Cell culture plasticware was acquired from Sarstedt Ltd. Human foetal osteoblasts (hFOB 1.19 (ATCC® CRL-11372™)) cell line was acquired from ATCC.

2.1. Cell culture

hFOB were maintained in DMEM/F12 supplemented with FBS (10%), L-glutamine (1%), and penicillin-streptomycin (1%). Incubation was at 34 °C and 5% CO_2. HUVEC were maintained in supplemented ECGM as per supplier's instruction at 37 °C and in 5% CO_2. Although this medium contains only 2% serum, some HUVEC experiments were performed under reduced serum conditions ($1/10^{th}$ standard cell culture supplement) to rule out an effect of endogenous S1P (Hanel et al., 2007).

2.2. Siponimod solution

Siponimod was dissolved in DMSO and then diluted in PBS as required. DMSO concentration were limited to <0.5% v/v in cell culture experiments. The potential toxicity of exceeding this concentration of DMSO was explored using hFOB and HUVEC cells ($2.5*10^4$ cell/well in 24 well plates) incubated with increasing concentrations of DMSO (0.32 - 3.2% in cell culture medium) for two and three days respectively. Thereafter, resazurin 60 µl of a 560 µM stock solution was added to wells for 3.5 hrs before acquiring fluorescence at excitation 488 nm/emission 595 nm.

2.3. Viability and proliferation

To estimate the effect of siponimod on cellular viability, cells were seeded at a density of $2.5*10^4$ cells per well in 24-well plates, the following day test drugs (100 nM siponimod or PBS vehicle) were added to cell culture medium. Following two- and three-days incubation (HUVEC and hFOB, respectively), 60 µl MTT solution (5 mg/ml stock) was added directly to wells and incubated for 2 h away from light. Wells were then rinsed with PBS. Formazan crystals were dissolved with DMSO and absorbance acquired at 570 nm using a Wallac Victor 2 plate reader (Perkin Elmer).

To determine the effect of siponimod on cellular proliferation, cells were seeded in 24-well plates at a density of $2.5*10^4$ cells per well. Siponimod (100 nM) or PBS vehicle were added to the cell culture medium for two- and three-days (HUVEC and hFOB, respectively). Thereafter, cells were detached using trypsin-EDTA 0.25%, diluted with cell culture medium, and individual well cell numbers manually counted using a haemocytometer. Additional cell counting experiments were conducted using hFOB cells maintained over 7 days (see section 2.4 for details)

As an additional measure of proliferation, cells were seeded in 96-well plates at densities of $1*10^4$ per well. Increased concentrations of siponimod, fingolimod, and S1P (all 1000 nM) were added the following day with fresh medium, and incubation continued for a further two days. Following treatment, BrdU was diluted in fresh medium and added to cells for 24 h. Thereafter cells were fixed for 30 min, then incubated for 90 min in a BrdU antibody solution, rinsed thoroughly with PBS followed by incubation with anti-BrdU substrate until sufficient colour development for plate reading at 405 nm.

2.4. Osteogenic differentiation

2.4.1. Para-nitrophenylphosphate

Alkaline phosphatase (ALP) is an early marker of osteoblast differentiation. *In vitro* osteoblast differentiation was estimated using para-nitrophenylphosphate (pNPP) as a substrate of alkaline phosphatase that is dephosphorylated into a yellow product (p-nitrophenol), detectable by absorbance at 405 nm.

hFOB cells ($5*10^4$) were seeded in 24-well plates and treated on day 0, 2, 4, and 6 with 1000 nM of either siponimod, fingolimod or S1P, with PBS vehicle as a control. Test agents were added directly to standard hFOB medium. As a positive differentiation control, cells were treated with osteogenic medium containing 50 µg/ml ascorbic acid and 7.5 mM β-Glycerophosphate. After 7 days, cells were detached with 100 µl trypsin-EDTA 0.25%, diluted with 200 µl fresh medium and counted using a haemocytometer. The cells were then transferred to 1.5 ml tubes and centrifuged at 3000 g for 5 min. Medium was aspirated from each tube and replaced with 100 µl pNPP substrate solution, allowing 30 min for yellow colour development. Absorbance was recorded at 405 nm using a Wallac Victor 2 plate reader (Perkin Elmer). The absorbance value of each sample was divided by its respective cell count, to normalize for differences due to cell numbers. Data are presented relative to the positive osteogenic medium control in each independent replicate.

2.4.2 Fast blue staining

Because the pNPP-based assay above does not allow the determination of the fraction of differentiating cells, as a complimentary measure of ALP, staining was performed using Fast Blue BB and Naphthol AS-MX phosphate. hFOB cells ($5*10^4$) were seeded in 24-well plates and treated every other day with siponimod (10-1000 nM), PBS, or osteogenic medium for 7 days. Thereafter, cells were equilibrated in an alkaline buffer followed by incubation with

fast blue dye for 60 min. Using a BX51 microscope (OLYMPUS), three images were acquired per well (with a 4x objective). Using ImageJ analysis software, the number of stained cells and total cells was manually counted and expressed as a percentage of the total cell number.

2.5. Migration

Cell migration assays were conducted for HUVEC and hFOB cells using the same techniques but using cell type specific media.

2.5.1. Wound healing (scratch) assay

Cells were seeded at $1*10^5$ cells/well in 24-well plates and grown overnight to produce a nearly confluent monolayer. A linear scratch was created by hand using a 1 ml pipette tip, wells were rinsed with PBS to remove debris and the cell culture medium was replaced as follows: for hFOBs, DMEM/F12 supplemented with 0.1% FBS was used to reduce serum bioactive lipid effects. Likewise, for HUVEC cells ECGM was supplemented with $1/10^{th}$ the usual supplement. Siponimod and S1P (delivered in 20 µl PBS) were then added directly to cell culture medium. Brightfield images (4x objective) were acquired immediately and after 8 h using a BX51 microscope (OLYMPUS). Using the associated software, Stream (OLYMPUS), the distance between the edges of the scratch wound was measured and the change over time attributed to cellular migration into the empty space.

2.5.2 Transwell migration

Transwell migration was conducted to assess chemotactic activity of S1P agents. Cells were seeded at $5*10^4$ cells in 100 µl of medium in the upper chamber of 8 µm pore poly ethylene terephthalate transwell inserts. Siponimod, S1P, or fingolimod (delivered in 20 µl PBS) were then added to the bottom chamber of the transwell system, which contained 600 µl of

medium. After 4, 8, or 24 h of incubation, culture medium was aspirated from the upper chamber, inserts were fixed with 10% NBF for 15 min at room temperature, then stained with 0.5% crystal violet for 30 min at room temperature. Thereafter inserts were rinsed with water to remove excess dye and the top side of the membrane was wiped with a cotton bud to remove non-migrated cells. Finally inserts were dried on the bench, before the membrane was visualized by light microscopy (BX43 microscope (OLYMPUS)). Five brightfield images per insert were acquired (10x objective), stained cells were manually counted using imageJ analysis software.

2.6. Cell attachment

The influence of siponimod on HUVEC attachment was investigated by seeding $5*10^4$ cells in 24 well plates using ECGM that was supplemented with $1/10^{th}$ standard supplement to reduce serum lipid effects. Siponimod and S1P (delivered in 20 µl PBS) were then added immediately to wells. After 4 h incubation, non-attached cells were removed by washing with PBS. Remaining cells were fixed with 10% NBF for 15 min, followed by staining with crystal violet 0.5% w/v for 30 min. Three brightfield images per well were acquired (10x objective), with stained cells manually counted using imageJ analysis software.

2.7. Cyclic AMP assay

The effect of siponimod on intracellular cAMP levels was determined using the cAMP-Glo™ Max Assay (Promega). hFOB cells were seeded at $2*10^4$ cells per well in 96 well plates and cultured overnight. Cells were washed with PBS, then treated with forskolin, siponimod, forskolin & siponimod combined, and a control containing the DMSO vehicle (concentration 0.32 %) for 1 h. All conditions included 500 µM IBMX to inhibit phosphodiesterases. Luminescence was measured and cAMP concentrations calculated using a standard curve as per the manufacturer’s protocol.

2.8. Statistical analysis

Results were expressed as mean ± standard deviation (S.D.), unless otherwise stated. Determining statistical significance was performed using one-way analysis of variance (ANOVA) followed by Bonferroni post-test for multiple comparisons. Differences were considered significant at $P < 0.05$. We used extra-sum-of-squares F tests as previously described (Waeber and Moskowitz, 1995) to determine whether drug responses were concentration-dependent (with the null hypothesis that data points were best fitted with a horizontal line, i.e. showed no concentration dependence).

3. Results

3.1. Siponimod solution

Siponimod was applied to cells in *in vitro* experiments as an aqueous solution of PBS containing a small concentration of DMSO as a cosolvent (0.32 % v/v). In order to determine whether the use of DMSO as a cosolvent would negatively impact hFOB and HUVEC cells used throughout this work, increasing concentrations of DMSO were applied to cells and their viability determined by resazurin assay (Fig 1). For hFOB cells there was no statistically significant change in cell viability when using 0.32 % DMSO compared to PBS control (91.5 ± 24.2 % compared to 100 ± 26.7 %). With increasing concentration of DMSO, cell viability trended downwards albeit without achieving statistical significance until a DMSO concentration of 3.22 % produced a significant fall in hFOB viability compared to PBS control and the 0.32 % condition (4.8 ± 2.7 % compared to 100 ± 26.7 % and 91.5 ± 24.2 %, $P < 0.05$). For HUVEC cells incubated with a concentration of 0.32 % DMSO there was no statistically significant change in cell viability over the experimental duration compared PBS control (99.4 ± 9.3 % compared 100 ± 4.2 %). As before DMSO showed a statistically significant reduction in cell viability at increased concentrations of 3.22 % compared to PBS and the 0.32 % condition (25.0 ± 12.1 % compared to 100 ± 4.2 % and 99.4 ± 9.3 %, $P < 0.05$)

Fig 1.

3.2. Viability and proliferation

Siponimod effect on cell viability and proliferation was investigated using hFOB and HUVEC cells. MTT assays were used to determine cell viability, with results presented as absorbance at 570 nm expressed as a percentage of positive control (for hFOBs, fully supplemented DMEM/F12, for HUVEC fully supplemented ECGM). Manual cell counting

was used to determine cell proliferation, with data presented as average cell numbers expressed as a percentage of positive control. Viability of hFOB cells treated with 100 nM siponimod were not significantly different to those treated with PBS vehicle (42.1 ± 7.6 % compared to 36.9 ± 8.6 %, ns), this lack of effect was also seen in manual cell counting experiments comparing 100 nM siponimod and PBS vehicle (49.1 ± 4.1 % compared to 44.9 ± 0.8 %, ns) (Fig 2 A & B). For HUVEC 100 nM siponimod produced no significant difference in viability compared to PBS vehicle (80.9 ± 8.8 % compared to 74.9 ± 8.2 %, ns). There was similarly no statistically significant change in manual cell count results between 100 nM siponimod and PBS vehicle (68.1 ± 12.7 % compared to 59.1 ± 12.7 %, ns) (Fig 2 C & D). Additionally, BrdU assay confirmed the absence of a proliferative effect for 1000 nM siponimod on both the hFOB cells and HUVEC (Fig 2 E & F). The BrdU assays also showed that there was no discernible effect on proliferation for either S1P or fingolimod (1000 nM).

Over a 7-day experimental duration (Fig 2 G), none of siponimod, fingolimod or S1P (all 1000 nM) led to any statistically significant change in hFOB cell count compared to PBS control (87.9 ± 16.5 % for siponimod, 88.7 ± 10.3 % for fingolimod, and 72.5 ± 18.7 % for S1P compared to 100 ± 37.1 % for PBS control). Likewise, increasing concentrations of siponimod (10-1000 nM (Fig 2 H)) did not show any statistically significant changes in cell number compared to PBS control (91.2 ± 5.0 % for 10 nM, 95.8 ± 15.5 % for 100 nM, and 82.2 ± 24.2 % for 1000 nM compared to 100 ± 14.7 % for PBS control).

Fig 2.

3.3. Osteogenic differentiation

3.3.1. Para-nitrophenylphosphate

hFOB cells were incubated in medium containing equal concentrations (1000 nM) of either siponimod, fingolimod, or S1P (Fig 3). Absorbance values for the ALP product p-nitrophenol

were normalised according to manual cell counts. Data is expressed as a percentage of the osteogenic medium positive control across each replicate. Fig 3 A shows the results of the comparison between the three investigated drugs (siponimod, fingolimod, and S1P). Whereas 1000 nM fingolimod showed no significant difference compared to PBS vehicle (44.8 ± 2.7 % compared to 39.8 ± 9.5 %), siponimod (1000 nM) increased absorbance/count compared to PBS vehicle (68.4 ± 9.7 % compared to 39.8 ± 9.5 %, $P < 0.05$). This increase was not significantly different from that induced by 1000nM S1P (78.1 ± 10.3 % compared to 39.8 ± 9.5 % for PBS vehicle, $P < 0.05$) and the response to siponimod ranging from 10-1000 nM was concentration dependent (F statistic = 11.46; P = 0.0069) (Fig 3 B).

Fig 3.

3.3.2. Fast blue staining

Alkaline phosphatase staining (Fig 4) was performed to complement the pNPP-based assessment above. Results represent the number of stained cells divided by the total number of cells, expressed as a percentage. hFOB cells were incubated with three concentrations of siponimod (10, 100, and 1000 nM). The concentrations 100 nM and 1000 nM resulted in an increased fraction of stained cells (100 nM siponimod 3.7 ± 0.6 ($P < 0.05$), and 1000 nM siponimod 4.2 ± 0.8 % ($P < 0.05$) compared to PBS vehicle 1.9 ± 0.6 %) and the response was concentration dependent (F statistic = 6.53; P = 0.038).

Fig 4.

3.4. Migration

3.4.1. Wound healing (scratch) assay

Scratch assays were performed to investigate whether the migratory response of hFOB and HUVEC cells was increased by siponimod. While hFOB cells did not respond to 100 nM siponimod after 8 h (Fig 5 A), HUVEC cells scratch wound closure was doubled in the

presence of 100 nM siponimod compared to PBS vehicle (45.8 ± 4.0 % compared to 22.5 ± 6.0 %, $P < 0.05$) (Fig 5 B). The concentration responsiveness of the effect was examined in a separate series of experiments; while all siponimod concentrations (1, 10, and 100 nM) produced a statistically significant increase in scratch wound closure compared to PBS vehicle (40.9 ± 5.0 %, 42.3 ± 3.5 %, and 45.9 ± 2.9 % compared to 22.7 ± 7.2 %, $P < 0.05$) (Fig 5 C), this response was found to not be concentration dependent (F statistic = 2.82; $P = 0.14$). The migratory response of HUVEC to 100 nM S1P was qualitatively similar to the effect of siponimod (Fig 5 D); 40.6 ± 3.6 % for S1P compared to 18.1 ± 3.5 % for PBS, $P < 0.05$. However, these experiments were conducted independently, precluding a direct comparison.

Fig 5.

3.4.2. Transwell migration

Following the data obtained from scratch wound assays, transwell migration assays were conducted to test the hypothesis that siponimod-enhanced migration of HUVEC was due to a chemotactic effect. Due to lack of scratch assay effect, hFOB cells were not investigated.

In transwell migration assays conducted under standard endothelial growth medium conditions (2 % v/v serum), 100 nM siponimod added to the bottom chamber of the transwell system resulted in a reduction in the number of migrated cells detected on the bottom side of the membrane compared to PBS vehicle (26.9 ± 7.4 % compared to 71.6 ± 10.3 %, $P < 0.05$) (Fig 6 A).

The concentration of S1P in serum is in the submicromolar range, i.e. sufficient to activate S1P receptors (Thuy et al., 2014). In contrast, much lower S1P concentrations are detected in tissues; this S1P gradient controls the trafficking of immune and hematopoietic stem progenitor cells (Liu et al., 2011). To test the hypothesis that the “repulsive” effect of

siponimod added to the bottom chamber under high serum concentrations was due to siponimod-induced receptor internalization, thereby blocking serum-induced cell migration, we tested the effects of S1P and siponimod added to the bottom chamber under reduced serum conditions (0.2% v/v serum). Under these conditions, 100 nM siponimod produced no statistically significant change in the number of migrated cells compared to PBS vehicle after 4 h (40.3 ± 11.0 % compared to 33.8 ± 10.1 %, ns) (Fig 6 B). S1P (100 nM) alone resulted in an increased number of migrated cells compared to PBS vehicle after 4 h (111.5 ± 19.5 % compared to 36.2 ± 16.7 %, $P < 0.05$) (Fig 6 C). When S1P was administered in combination with 100 nM siponimod, the number of migrated cells was significantly reduced (20.4 ± 22.8 % compared to 111.5 ± 19.5 %, $P < 0.05$) (Fig 6 C).

We then performed transwell migration assays over 8 h to more closely match scratch assay conditions. Here 100 nM siponimod produced a statistically significant increase in the number of migrated cells compared to PBS vehicle (34.7 ± 7.9 % compared to 10.8 ± 3.3 %, $P < 0.05$) (Fig 6 D). As in the 4 h experiment, 100 nM S1P increased the number of migrated cells compared PBS vehicle (106.3 ± 11.9 % compared to 10.8 ± 3.3 %, $P < 0.05$), an effect that was antagonised by 100 nM siponimod (106.3 ± 8.0 % compared to 16.8 ± 7.3 %, $P < 0.05$) (Fig 6 D).

Migration over 24 h was investigated (Fig 6 E) and showed a substantial fall in the overall number of migrating cells compared to experiments conducted at 4 and 8 h.

Fig 6.

3.5. Cell attachment

To further rule out the possibility that the siponimod-induced reduction of HUVEC migration (Fig 6 A) was caused by an effect on cell attachment, we examined the effect of various test agents on this parameter. Alone, 100 nM siponimod resulted in no statistically significant

change in cell attachment compared to PBS vehicle (67.0 ± 0.6 % compared to 58.6 ± 5.0 %, ns). S1P (100 nM) resulted in a statistically significant increase in cell attachment compared to PBS vehicle (88.4 ± 6.4 % compared to 58.6 ± 5.0 %, $P < 0.05$). This effect was antagonised when 100 nM siponimod was added with 100 nM S1P (88.4 ± 6.4 % attachment for S1P compared to 51.3 ± 2.7 % for siponimod/S1P, $P < 0.05$). Attachment in the presence of siponimod and S1P was not statistically different from attachment in the PBS vehicle condition (51.3 ± 2.7 % compared to 58.6 ± 5.0 %, ns).

Fig 7.

3.6. Cyclic AMP assay

Intracellular cAMP was quantified in an attempt to confirm the identity of the S1P receptor involved and to examine potential signalling mechanisms involved in the response to siponimod. Results showed that after 1 h, siponimod significantly inhibited forskolin-stimulated increases in intracellular cAMP (30.0% ± 22.9% for 1 μM forskolin + 100 nM siponimod compared to 100 % ± 11.5 % for 1 μM forskolin, $P < 0.05$) (Fig 8). Siponimod alone did not lead to any significant change in baseline cAMP (12.6 ± 8.6 % for 100 nM siponimod compared to 10.2 ± 10.1 % for untreated control).

Fig 8.

4. Discussion

The overall aim of these studies was to assess the suitability of siponimod as a potential bone regenerative agent, to be eluted by a localised delivery device to stimulate repair in critical bone defects. With this goal in mind, we investigated the effect of siponimod on osteoblast and endothelial cells proliferation, differentiation and migration. Primarily, it was necessary to show that solutions of siponimod, prepared using DMSO as a co-solvent, did not

352 negatively impact cell viability. Therefore, experiments were conducted showing that the
353 concentration of DMSO used (0.32 %) was non-toxic in both hFOB cells and HUVEC. This
354 concurs with the literature, that a concentration less than 0.5 % should not impact cell
355 viability (Shah et al., 2019). Shifting focus to the viability assays proper, S1P is well
356 established in promoting endothelial cell proliferation, viability and survival, likely via the
357 $S1P_1$ or $S1P_3$ receptors (Kwon et al., 2001; Lee et al., 2000; Lee et al., 1999; Rikitake et al.,
358 2002; Wang et al., 1999). Therefore, the lack of proliferative effect herein, as well as
359 siponimod's selectivity for receptors 1 and 5 may indicate that the $S1P_3$ receptor plays the
360 more important role. Another possibility is that siponimod is behaving like fingolimod, which
361 at concentrations below 250 nM has no effect on HUVEC viability but exhibits toxicity
362 above 250 nM (Schmid et al., 2007). Siponimod also had no effect on osteoblast
363 proliferation, perhaps explained by a possible role for siponimod in osteoblast differentiation,
364 pushing the cells towards a post-mitotic phase precluding extensive proliferation (Long,
365 2011).

366 ALP is commonly used as a marker of osteoblast differentiation. Here we show that exposure
367 to siponimod (but not to fingolimod) increased ALP activity, an effect equivalent to that seen
368 with the same concentration of S1P. Complementary ALP staining showed a corresponding
369 siponimod-induced increase in the number of stained cells. S1P and fingolimod have
370 previously been shown to increase markers of osteoblast differentiation as well as stimulating
371 the osteogenic differentiation pathway of osteoblasts (Brizuela et al., 2014; Lotinun et al.,
372 2013; Matsuzaki et al., 2013; Sato et al., 2012) and mesenchymal stems cells (Hashimoto et
373 al., 2016; Hashimoto et al., 2015; Marycz et al., 2016; Pederson et al., 2008), but it is unclear
374 whether $S1P_1$, $S1P_3$ or both receptor subtypes mediate these effects. Studies of S1P on
375 osteoblast differentiation with receptor antagonists have shown an exclusive role for $S1P_3$ in
376 osteoblast maturation (Brizuela et al., 2014), whereas $S1P_1$ receptors were shown to mediate

the effect of S1P and fingolimod on osteoblast differentiation, when used in conjunction with bone morphogenetic protein 2 (Sato et al., 2012). There is conflicting evidence regarding the effect of fingolimod, which has recently been shown to reduce markers of bone formation (including ALP) in osteoblasts and chondrocytes (El Jamal et al., 2019). This study, which is more in line with our findings with fingolimod, taken together with the effects presented herein for siponimod, an $S1P_{1/5}$ selective modulator, and the lack of detectable $S1P_5$ receptor mRNA expression in pre-osteoblasts and osteoblasts (Roelofsen et al., 2008), suggest that $S1P_1$ receptor stimulation is sufficient to induce osteoblast differentiation.

S1P is known to stimulate the migration of osteoblast precursors, osteoclasts, and endothelial cells (Lee et al., 2000; Lee et al., 1999; Ohmori et al., 2001; Pederson et al., 2008; Roelofsen et al., 2008; Ryu et al., 2002). Here we found that siponimod had no effect on the migration of hFOB osteoblasts. This lack of effect suggests that previously reported effects of S1P on osteoblast migration were mediated by a receptor other than $S1P_1$ or $S1P_5$, or that this effect was dependent on the differentiation stage. While both $S1P_1$ and $S1P_2$ receptors have been shown to regulate the migration of cells of the osteoblast lineage, they only did so in MC3T3-E1 pre-osteoblasts (Roelofsen et al., 2008). Upon reaching cell confluence, cultures of hFOB cells express high levels of phenotypic markers associated with osteoblast differentiation (Harris et al., 1995). It is therefore possible that the cells used in our studies were more differentiated than the pre-osteoblasts known to migrate in response to S1P, although the relatively small fraction of cells expressing ALP in our studies, even after one-week exposure to osteogenic medium, would seem to argue against this explanation, leaving open the possibility that species differences may account for the discrepant migration response in hFOB (of human origin) and in murine MC3T3-E1 cells. Our studies did however show a significant effect on endothelial cell migration, doubling HUVEC cell motility in scratch assays. The effect of siponimod was found to be similar to that of S1P (Lee et al., 2000; Lee

et al., 1999; Ohmori et al., 2001; Ryu et al., 2002). However, the extent of this response did not seem to depend on siponimod's concentration (1-100 nM). It is possible that a concentration response relationship may have emerged with further independent experiments. Alternatively, the effect may already have been maximal at 1 nM siponimod, reaching a plateau thereafter. Indeed, siponimod is a potent and efficacious $S1P_1$ agonist, with subnanomolar EC_{50} in [^{35}S]GTPγS binding assays (Gergely et al., 2012; Lukas et al., 2014). However, while siponimod is often tested at 100 nM in published functional cell culture experiments (Gentile et al., 2016; Lupino et al., 2019), we found only two reports showing a concentration response curve in such preparations, in which siponimod mediated a response with an EC50 of 15.8 nM (Gergely et al., 2012) and only showed a non-significant trend at 1 nM (O'Sullivan et al., 2016).

In transwell assays designed to test whether the effect of siponimod in the scratch assay was due to increased chemokinesis or to chemotaxis, siponimod decreased the migration of endothelial cells under standard growth medium conditions (2% v/v serum). We hypothesized that siponimod may have internalized S1P receptors, blocking the effect of S1P present in the growth medium. Indeed, when transwell assays were conducted under low serum conditions (0.2% v/v serum), siponimod had no significant effect on cell migration, and S1P stimulated endothelial cell migration in a siponimod-sensitive manner and as effectively as serum.

To understand how siponimod interfered with S1P-mediated transwell migration, cell attachment studies performed under similar conditions to the transwell assays showed that siponimod interfered with S1P-mediated increases in cell attachment over 4 h. It is therefore possible that decreased cell attachment may have contributed to the reduced transwell migration observed after 4 h. Given that the effect of siponimod in scratch assays was determined over 8 hr, additional 8 hr transwell assays were conducted and showed that while siponimod still antagonised S1P mediated migration, it also induced a statistically significant

increase in cell migration when added on its own, albeit with an effect 3-fold weaker than the effect of S1P. This may be due to persistent signalling after internalisation of the $S1P_1$ receptor (Mullershausen et al., 2009), which may only lead to migration after long exposure (8 h) to siponimod, but not after 4 h, and may also indicate that siponimod behaves similarly to fingolimod, which has been shown to induce cellular motility in scratch assays (Mullershausen et al., 2009) but impede HUVEC migration across a membrane (Ho et al., 2005; LaMontagne et al., 2006; Tanaka et al., 2013). The same experiments were conducted over 24 h, however the substantial drop in the number of cells migrating indicated that the extended experimental duration under low serum conditions may have impacted HUVEC viability.

The role of intracellular cAMP in bone remodelling and bone cell differentiation has long been known (Rodan et al., 1975), but the relationship is complex. While some early studies have shown that parathyroid hormone stimulate the *in vitro* differentiation of osteoblasts via intracellular cAMP production (Nakatani et al., 1984), other reports show that the influence of cAMP on ALP expression changes depending on the stage of osteoblast differentiation, and parathyroid hormone may preferentially inhibit the differentiation of more mature osteoblasts (Isogai et al., 1996). Expanding on the complexity of the relation between cAMP and osteoblast differentiation markers, increasing levels of cAMP have been shown to result in decreased ALP but increased osteocalcin expression (Romanello et al., 2001). More recently, increasing cAMP levels have been shown to suppress osteoblast mineralisation (Nishihara et al., 2018). Forskolin-induced cAMP is known to be inhibited by both sphingosine 1-phosphate and fingolimod after 1 h incubation (Mullershausen et al., 2009), with results similar to those shown for siponimod. This effect is most likely associated with the inhibitory Gi protein coupled to the $S1P_1$ receptor, which is the mechanism through which S1P and fingolimod produce the same inhibitory effect. Based on the somewhat

contradictory existing literature, it is not straightforward to provide a mechanism linking the adenylate cyclase inhibiting effect of siponimod on our hFOB osteoblasts and the effects of this agent on hFOB cell differentiation. However, we hypothesize that siponimod may maintain a chronically low level of intracellular cAMP through its interaction with $S1P_1$ receptors, resulting in increased ALP activity, indicative of increased osteoblast differentiation.

Fingolimod, and now siponimod, both antagonise the chemotactic effect of S1P on endothelial cells. Fingolimod has shown proangiogenic effects *in vivo*, ultimately improving recovery of bone defects (Huang et al., 2012; Li et al., 2019). Therefore, given siponimod's effect on osteoblast differentiation, it may be useful to incorporate siponimod into a localised delivery device to investigate the effects of siponimod *in vivo* towards the same end.

One of the limitations of the current study is that it does not consider osteoclasts, or the coupling between osteoblasts and osteoclasts (Pederson et al., 2008). This communication is known to involve S1P receptors and would likely impact significantly on healing outcomes in any potential *in vivo* studies. Also, our ALP staining studies showed that the total fraction of stained cells was relatively small, being less than 10% of the total number of cells. This may be due to the use of a relatively early time point for analysis (7 days). Conducting the experiment over a longer duration, more consistent with the effect of a drug eluting scaffold (Das et al., 2014a; Das et al., 2014b) may have led to a more meaningful effect on differentiation.

5. Conclusion

The aim of this work was to investigate the potential of siponimod in a bone regenerative context, ultimately towards its use in conditions of critical bone defects, as part of a localised delivery device, but improving on the specificity of the eluted drug (Das et al., 2014a; Das et

al., 2014b; Huang et al., 2012; Li et al., 2019). These studies add to the relatively small amount of literature on the functional effects of siponimod in cell culture models. In the context of bone repair, the differentiation effect of siponimod on osteoblasts, taken together with its effects on endothelial cells suggest that this selective $S1P_1$ modulator may be useful, particularly in conditions of critical defects that remain a significant therapeutic challenge. However, more robust *in vivo* experiments would be the next step before making any determinative conclusions.

Bibliography

Behrangi, N., Fischbach, F., Kipp, M., 2019. Mechanism of Siponimod: Anti-Inflammatory and Neuroprotective Mode of Action. Cells 8.

Brinkmann, V., Billich, A., Baumruker, T., Heining, P., Schmouder, R., Francis, G., Aradhye, S., Burtin, P., 2010. Fingolimod (FTY720): discovery and development of an oral drug to treat multiple sclerosis. Nat Rev Drug Discov 9, 883-897.

Brizuela, L., Martin, C., Jeannot, P., Ader, I., Gstalder, C., Andrieu, G., Bocquet, M., Laffosse, J.M., Gomez-Brouchet, A., Malavaud, B., Sabbadini, R.A., Cuvillier, O., 2014. Osteoblast-derived sphingosine 1-phosphate to induce proliferation and confer resistance to therapeutics to bone metastasis-derived prostate cancer cells. Molecular Oncology 8, 1181-1195.

Cugati, S., Chen, C.S., Lake, S., Lee, A.W., 2014. Fingolimod and macular edema: Pathophysiology, diagnosis, and management. Neurol Clin Pract 4, 402-409.

Das, A., Barker, D.A., Wang, T., Lau, C.M., Lin, Y., Botchwey, E.A., 2014a. Delivery of bioactive lipids from composite microgel-microsphere injectable scaffolds enhances stem cell recruitment and skeletal repair. PLoS One 9, e101276.

Das, A., Tanner, S., Barker, D.A., Green, D., Botchwey, E.A., 2014b. Delivery of S1P receptor-targeted drugs via biodegradable polymer scaffolds enhances bone regeneration in a critical size cranial defect. J Biomed Mater Res A 102, 1210-1218.

DiMarco, J.P., O'Connor, P., Cohen, J.A., Reder, A.T., Zhang-Auberson, L., Tang, D., Collins, W., Kappos, L., 2014. First-dose effects of fingolimod: Pooled safety data from three phase 3 studies. Mult Scler Relat Disord 3, 629-638.

El Jamal, A., Briolay, A., Mebarek, S., Le Goff, B., Blanchard, F., Magne, D., Brizuela, L., Bougault, C., 2019. Cytokine- and stretch-induced sphingosine1-phosphate production by enthesis cells could favor abnormal ossification in spondyloarthritis. J Bone Miner Res.

Gentile, A., Musella, A., Bullitta, S., Fresegna, D., De Vito, F., Fantozzi, R., Piras, E., Gargano, F., Borsellino, G., Battistini, L., Schubart, A., Mandolesi, G., Centonze, D., 2016. Siponimod (BAF312) prevents synaptic neurodegeneration in experimental multiple sclerosis. J Neuroinflammation 13, 207.

Gergely, P., Nuesslein-Hildesheim, B., Guerini, D., Brinkmann, V., Traebert, M., Bruns, C., Pan, S., Gray, N.S., Hinterding, K., Cooke, N.G., Groenewegen, A., Vitaliti, A., Sing, T., Luttringer, O., Yang, J., Gardin, A., Wang, N., Crumb, W.J., Saltzman, M., Rosenberg, M., Wallstrom, E., 2012. The selective sphingosine 1-phosphate receptor modulator BAF312 redirects lymphocyte distribution and has species-specific effects on heart rate. Brit J Pharmacol 167, 1035-1047.

Hanel, P., Andreani, P., Graler, M.H., 2007. Erythrocytes store and release sphingosine 1-phosphate in blood. FASEB journal : official publication of the Federation of American Societies for Experimental Biology 21, 1202-1209.

Harris, S.A., Enger, R.J., Riggs, B.L., Spelsberg, T.C., 1995. Development and characterization of a conditionally immortalized human fetal osteoblastic cell line. J Bone Miner Res 10, 178-186.

Hashimoto, Y., Kobayashi, M., Matsuzaki, E., Higashi, K., Takahashi-Yanaga, F., Takano, A., Hirata, M., Nishimura, F., 2016. Sphingosine-1-phosphate-enhanced Wnt5a promotes osteogenic differentiation in C3H10T1/2 cells. Cell Biology International 40, 1129-1136.

Hashimoto, Y., Matsuzaki, E., Higashi, K., Takahashi-Yanaga, F., Takano, A., Hirata, M., Nishimura, F., 2015. Sphingosine-1-phosphate inhibits differentiation of C3H10T1/2 cells into adipocyte. Mol Cell Biochem 401, 39-47.

Heilmann, A., Schinke, T., Bindl, R., Wehner, T., Rapp, A., Haffner-Luntzer, M., Liedert, A., Amling, M., Ignatius, A., 2013. Systemic treatment with the sphingosine-1-phosphate analog FTY720 does not improve fracture healing in mice. J Orthop Res 31, 1845-1850.
Hla, T., 2004. Physiological and pathological actions of sphingosine 1-phosphate. Semin Cell Dev Biol 15, 513-520.
Ho, J.W., Man, K., Sun, C.K., Lee, T.K., Poon, R.T., Fan, S.T., 2005. Effects of a novel immunomodulating agent, FTY720, on tumor growth and angiogenesis in hepatocellular carcinoma. Mol Cancer Ther 4, 1430-1438.
Huang, C., Das, A., Barker, D., Tholpady, S., Wang, T., Cui, Q.J., Ogle, R., Botchwey, E., 2012. Local delivery of FTY720 accelerates cranial allograft incorporation and bone formation. Cell and Tissue Research 347, 553-566.
Isogai, Y., Akatsu, T., Ishizuya, T., Yamaguchi, A., Hori, M., Takahashi, N., Suda, T., 1996. Parathyroid hormone regulates osteoblast differentiation positively or negatively depending on the differentiation stages. J Bone Miner Res 11, 1384-1393.
Kwon, Y.G., Min, J.K., Kim, K.M., Lee, D.J., Billiar, T.R., Kim, Y.M., 2001. Sphingosine 1-phosphate protects human umbilical vein endothelial cells from serum-deprived apoptosis by nitric oxide production. J Biol Chem 276, 10627-10633.
LaMontagne, K., Littlewood-Evans, A., Schnell, C., O'Reilly, T., Wyder, L., Sanchez, T., Probst, B., Butler, J., Wood, A., Liau, G., Billy, E., Theuer, A., Hla, T., Wood, J., 2006. Antagonism of sphingosine-1-phosphate receptors by FTY720 inhibits angiogenesis and tumor vascularization. Cancer Res 66, 221-231.
Lee, H., Goetzl, E.J., An, S., 2000. Lysophosphatidic acid and sphingosine 1-phosphate stimulate endothelial cell wound healing. Am J Physiol Cell Physiol 278, C612-618.
Lee, O.H., Kim, Y.M., Lee, Y.M., Moon, E.J., Lee, D.J., Kim, J.H., Kim, K.W., Kwon, Y.G., 1999. Sphingosine 1-phosphate induces angiogenesis: its angiogenic action and signaling mechanism in human umbilical vein endothelial cells. Biochem Biophys Res Commun 264, 743-750.
Li, S., Song, C., Yang, S., Yu, W., Zhang, W., Zhang, G., Xi, Z., Lu, E., 2019. Supercritical CO2 foamed composite scaffolds incorporating bioactive lipids promote vascularized bone regeneration via Hif-1alpha upregulation and enhanced type H vessel formation. Acta Biomater 94, 253-267.
Liu, J., Hsu, A., Lee, J.F., Cramer, D.E., Lee, M.J., 2011. To stay or to leave: Stem cells and progenitor cells navigating the S1P gradient. World J Biol Chem 2, 1-13.
Long, F., 2011. Building strong bones: molecular regulation of the osteoblast lineage. Nat Rev Mol Cell Biol 13, 27-38.
Lotinun, S., Kiviranta, R., Matsubara, T., Alzate, J.A., Neff, L., Luth, A., Koskivirta, I., Kleuser, B., Vacher, J., Vuorio, E., Horne, W.C., Baron, R., 2013. Osteoclast-specific cathepsin K deletion stimulates S1P-dependent bone formation. Journal of Clinical Investigation 123, 666-681.
Lukas, S., Patnaude, L., Haxhinasto, S., Slavin, A., Hill-Drzewi, M., Horan, J., Modis, L.K., 2014. No Differences Observed among Multiple Clinical S1P(1) Receptor Agonists (Functional Antagonists) in S1P(1) Receptor Down-regulation and Degradation. J Biomol Screen 19, 407-416.
Lupino, L., Perry, T., Margielewska, S., Hollows, R., Ibrahim, M., Care, M., Allegood, J., Tooze, R., Sabbadini, R., Reynolds, G., Bicknell, R., Rudzki, Z., Lin Hock, Y., Zanetto, U., Wei, W., Simmons, W., Spiegel, S., Woodman, C.B.J., Rowe, M., Vrzalikova, K., Murray, P.G., 2019. Sphingosine-1-phosphate signalling drives an angiogenic transcriptional programme in diffuse large B cell lymphoma. Leukemia.
Marycz, K., Krzak, J., Maredziak, M., Tomaszewski, K.A., Szczurek, A., Moszak, K., 2016. The influence of metal-based biomaterials functionalized with sphingosine-1-phosphate on the

cellular response and osteogenic differentaion potenial of human adipose derived mesenchymal stem cells invitro. Journal of Biomaterials Applications 30, 1517-1533.
Matsuzaki, E., Hiratsuka, S., Hamachi, T., Takahashi-Yanaga, F., Hashimoto, Y., Higashi, K., Kobayashi, M., Hirofuji, T., Hirata, M., Maeda, K., 2013. Sphingosine-1-phosphate promotes the nuclear translocation of beta-catenin and thereby induces osteoprotegerin gene expression in osteoblast-like cell lines. Bone 55, 315-324.
Mullershausen, F., Zecri, F., Cetin, C., Billich, A., Guerini, D., Seuwen, K., 2009. Persistent signaling induced by FTY720-phosphate is mediated by internalized S1P1 receptors. Nat Chem Biol 5, 428-434.
Nakatani, Y., Tsunoi, M., Hakeda, Y., Kurihara, N., Fujita, K., Kumegawa, M., 1984. Effects of parathyroid hormone on cAMP production and alkaline phosphatase activity in osteoblastic clone MC3T3-E1 cells. Biochem Biophys Res Commun 123, 894-898.
Nishihara, S., Ikeda, M., Ozawa, H., Akiyama, M., Yamaguchi, S., Nakahama, K.I., 2018. Role of cAMP in phenotypic changes of osteoblasts. Biochem Biophys Res Commun 495, 941-946.
O'Sullivan, C., Schubart, A., Mir, A.K., Dev, K.K., 2016. The dual S1PR1/S1PR5 drug BAF312 (Siponimod) attenuates demyelination in organotypic slice cultures. J Neuroinflammation 13, 31.
Ohmori, T., Yatomi, Y., Okamoto, H., Miura, Y., Rile, G., Satoh, K., Ozaki, Y., 2001. G(i)-mediated Cas tyrosine phosphorylation in vascular endothelial cells stimulated with sphingosine 1-phosphate: possible involvement in cell motility enhancement in cooperation with Rho-mediated pathways. J Biol Chem 276, 5274-5280.
Pederson, L., Ruan, M., Westendorf, J.J., Khosla, S., Oursler, M.J., 2008. Regulation of bone formation by osteoclasts involves Wnt/BMP signaling and the chemokine sphingosine-1-phosphate. Proc Natl Acad Sci U S A 105, 20764-20769.
Rikitake, Y., Hirata, K., Kawashima, S., Ozaki, M., Takahashi, T., Ogawa, W., Inoue, N., Yokoyama, M., 2002. Involvement of endothelial nitric oxide in sphingosine-1-phosphate-induced angiogenesis. Arterioscler Thromb Vasc Biol 22, 108-114.
Rodan, G.A., Bourret, L.A., Harvey, A., Mensi, T., 1975. Cyclic AMP and cyclic GMP: mediators of the mechanical effects on bone remodeling. Science 189, 467-469.
Roelofsen, T., Akkers, R., Beumer, W., Apotheker, M., Steeghs, I., van de Ven, J., Gelderblom, C., Garritsen, A., Dechering, K., 2008. Sphingosine-1-Phosphate Acts as a Developmental Stage Specific Inhibitor of Platelet-Derived Growth Factor-induced Chemotaxis of Osteoblasts. Journal of Cellular Biochemistry 105, 1128-1138.
Romanello, M., Moro, L., Pirulli, D., Crovella, S., D'Andrea, P., 2001. Effects of cAMP on intercellular coupling and osteoblast differentiation. Biochem Biophys Res Commun 282, 1138-1144.
Ryu, Y., Takuwa, N., Sugimoto, N., Sakurada, S., Usui, S., Okamoto, H., Matsui, O., Takuwa, Y., 2002. Sphingosine-1-phosphate, a platelet-derived lysophospholipid mediator, negatively regulates cellular Rac activity and cell migration in vascular smooth muscle cells. Circ Res 90, 325-332.
Salomone, S., Waeber, C., 2011. Selectivity and specificity of sphingosine-1-phosphate receptor ligands: caveats and critical thinking in characterizing receptor-mediated effects. Front Pharmacol 2, 9.
Sartawi, Z., Schipani, E., Ryan, K.B., Waeber, C., 2017. Sphingosine 1-phosphate (S1P) signalling: Role in bone biology and potential therapeutic target for bone repair. Pharmacol Res 125, 232-245.
Sato, C., Iwasaki, T., Kitano, S., Tsunemi, S., Sano, H., 2012. Sphingosine 1-phosphate receptor activation enhances BMP-2-induced osteoblast differentiation. Biochemical and Biophysical Research Communications 423, 200-205.

Schmid, G., Guba, M., Ischenko, I., Papyan, A., Joka, M., Schrepfer, S., Bruns, C.J., Jauch, K.W., Heeschen, C., Graeb, C., 2007. The immunosuppressant FTY720 inhibits tumor angiogenesis via the sphingosine 1-phosphate receptor 1. J Cell Biochem 101, 259-270.
Shah, A.A., Gourishetti, K., Nayak, Y., 2019. Osteogenic Activity of Resveratrol in Human Fetal Osteoblast Cells. Pharmacogn Mag 15, 250-255.
Spiegel, S., Milstien, S., 2000. Sphingosine-1-phosphate: signaling inside and out. FEBS letters 476, 55-57.
Tanaka, Y., Okabe, S., Tauchi, T., Ito, Y., Umezu, T., Ohyashiki, J.H., Ohyashiki, K., 2013. Therapeutic Potential Of Targeting Sphingosine-1-Phosuphate and Sphingosine Kinases In Multiple Myeloma. Blood 122.
Thuy, A.V., Reimann, C.M., Hemdan, N.Y., Graler, M.H., 2014. Sphingosine 1-phosphate in blood: function, metabolism, and fate. Cell Physiol Biochem 34, 158-171.
Waeber, C., 2013. Sphingosine 1-Phosphate (S1P) Signaling and the Vasculature, in: Chun, J., Hla, T., Spiegel, S., Moolenaar, W. (Eds.), Lysophospholipid Receptors: Signaling and Biochemistry John Wiley & Sons Ltd, Hoboken, NJ, pp. 313-347.
Waeber, C., Moskowitz, M.A., 1995. [3H]sumatriptan labels both 5-HT1D and 5-HT1F receptor binding sites in the guinea pig brain: an autoradiographic study. Naunyn Schmiedebergs Arch Pharmacol 352, 263-275.
Wang, F., Van Brocklyn, J.R., Hobson, J.P., Movafagh, S., Zukowska-Grojec, Z., Milstien, S., Spiegel, S., 1999. Sphingosine 1-phosphate stimulates cell migration through a G(i)-coupled cell surface receptor. Potential involvement in angiogenesis. J Biol Chem 274, 35343-35350.

Fig 1. Viability assay for hFOB and HUVEC cells incubated with increasing concentrations of DMSO. (A) hFOB resazurin assay after 72 h, (B) HUVEC resazurin assay after 48 h. Data is expressed as a percentage of PBS control and is presented as mean ± S.D. from 3 independently repeated experiments (with 3 technical replicates). For hFOB cells, increasing DMSO concentrations were added to cell culture medium containing $1/10^{th}$ standard serum supplement. For HUVEC, DMSO concentrations were added to cell culture medium containing $1/3^{rd}$ standard supplements. Statistical analysis was performed by one-way ANOVA. There was no statistically significant difference between any group except for 3.22% DMSO, which was statistically different from all other groups (***: $P < 0.001$).

Fig 2. Viability and proliferation assays for hFOB and HUVEC cells. (A & B) hFOB MTT assay and cell count after 72 h, n=3 (4 technical replicates) (C & D) HUVEC MTT assay and cell count after 48 h, n=3 (4 technical replicates) (E & F) hFOB and HUVEC BrdU assay, n=3 (4 technical replicates) (G & H) hFOB cell count after 7 days incubation, n=4 (3 technical replicates). For A-F, data is expressed as a percentage (positive control set to 100%), for G & H data is expressed as a percentage of PBS control. For hFOB cells (in A-F), factors were added to cell culture medium containing 1/10th standard serum supplement, with standard growth medium (DMEM/F12) acting as positive control. For HUVEC (in A-F), factors were added to cell culture medium containing 1/3rd standard supplements, with standard growth medium (ECGM, containing 2% serum) acting as positive control. In G & H growth medium supplement was not altered. ‘’n=’’ represents the number of independently repeated experiments. Data is presented as mean ± S.D., statistical analysis by one-way ANOVA. NS: No statistical significance. *: $P < 0.05$. **: $P < 0.01$. ***: $P < 0.001$.

Fig 3. Alkaline phosphatase activity as an early marker of differentiation in hFOB cells. (A) Effect of siponimod, fingolimod, and S1P (1000 nM) after 7 days, n=4 (3 technical replicates) (B) Siponimod concentration response over 10-1000 nM after 7 days, n=4 (3

technical replicates). For A & B, data represents pNPP absorbance at 405 nm divided by cell count, relative to the positive control (osteogenic medium containing 50 µg/ml ascorbic acid & 7.5 mM β-glycerophosphate) in each independent replicate. ‘’n=’’ represents the number of independently repeated experiments. Data is presented as mean ± S.D., statistical analysis by one-way ANOVA. NS: No statistical significance. *: $P < 0.05$. **: $P < 0.01$. ***: $P < 0.001$.

Fig 4. Alkaline phosphatase (ALP) staining as an early marker of differentiation in hFOB cells. (A) Response to 10-1000 nM siponimod after 7 days, n=4 (3 technical replicates). Data represents the average number of manually counted Fast blue-stained cells divided by the total cell number. Osteogenic medium (containing 50 µg/ml ascorbic acid & 7.5 mM β-glycerophosphate) was used as a positive control. ‘’n=’’ represents the number of independently repeated experiments. Data is presented as mean ± S.D. Statistical analysis was done using one-way ANOVA. NS: No statistical significance. *: $P < 0.05$. **: $P < 0.01$. ***: $P < 0.001$. The percentage of ALP-stained cells in the presence of osteogenic medium was significantly different from the percentage of stained cells in all other conditions ($P < 0.001$). B, C, and D are representative brightfield photomicrographs of hFOB cells exposed to PBS (B), 100 nM siponimod (C), and osteogenic medium (D); blue cells are cells with higher alkaline phosphatase activity, and hence a higher level of differentiation. Scale bar is 500 µm.

Fig 5. Wound healing (scratch) assay for hFOB and HUVEC cells. (A) Effect of 100 nM siponimod on hFOB cells, n=4 (3 technical replicates), (B) Effect of 100 nM siponimod on HUVEC cells, n=7 (3 technical replicates), (C) Siponimod concentration response over 1-100 nM on HUVEC cells, n=3 (3 technical replicates); (D) Effect of 100 nM S1P on HUVEC, n=2 (3 technical replicates). Data represents the percentage closure of the scratch wound after 8 h. ‘’n=’’ represents the number of independently repeated experiments. Data is presented as

mean ± S.D., statistical analysis by one-way ANOVA. *: P < 0.05. **: P < 0.01. ***: P < 0.001. E-J: Representative photomicrographs for the experiment shown in (B) are shown at 0 and 8 h: (E,H) vehicle (PBS) control, (F, I) positive control (FBS), and (G, J) 100 nM siponimod. The white arrowheads at the top and bottom of each photomicrograph show the edge of the manually created scratch wound. Images were acquired using a 4x objective, scale bars are 500 µm.

Fig 6. Transwell migration assay for HUVEC cells. (A) Effect of 100 nM siponimod under standard growth medium conditions (2 % serum) over 4 h, n=4 (3 technical replicates) (B) Effect of 100 nM siponimod under reduced serum conditions ($1/10^{th}$ standard cell culture supplement containing 0.2 % serum) over 4 h, n=5 (3 technical replicates) (C) Effect of 100 nM S1P alone and combined with 100 nM siponimod under reduced serum conditions for 4 h, n=3 (3 technical replicates) (D) Effect of 100 nM siponimod under reduced serum conditions over 8 h, n=5 (2 technical replicates) (E) migration over 24 h, n=3 (2 technical replicates. Data, presented as mean ± S.D., represents the number of cells counted on the bottom side of a transwell membrane, expressed as a percentage (positive control set to 100%). ‘’n=’’ represents the number of independently repeated experiments. Statistical analysis by one-way ANOVA; ns: No statistical significance. **: P < 0.01. ***: P < 0.001. (F-I) Representative photomicrographs for experimental conditions shown in (D): FBS (F), PBS (G), 100 nM siponimod (H) and 100 nM siponimod + 100 nM S1P (I). Scale bar: 500 µm.

Fig 7. Cell attachment assay for HUVEC cells. Effect of siponimod, S1P, and siponimod + S1P (all 100 nM) on cell attachment after 4 h incubation under reduced serum conditions, n=3 (2 technical replicates. Data, presented as mean ± S.D., represents the number of cells attached to the well, expressed as a percentage (positive control set to 100%). ‘’n=’’ represents the number of independently repeated experiments. Statistical analysis by one-way

ANOVA. NS: No statistical significance. ***: P < 0.001). (B-E) Representative images for experimental conditions shown in cell attachment assay: FBS (B), PBS (C), 100 nM siponimod (D) and 100 nM siponimod + 100 nM S1P (E). Scale bar: 500 µm.

Fig 8. Effects of siponimod on intracellular cAMP in hFOB cells. The effect of 100 nM siponimod alone and in combination with 1 µM forskolin, n=4 (3 technical replicates). Cells were incubated in the presence of the indicated drugs for 1 h. Data, presented as mean ± S.D., represents the concentration of intracellular cAMP, expressed relative to 1 µM forskolin. ‘’n=’’ represents the number of independently repeated experiments. Statistical analysis by one-way ANOVA. ***: P < 0.001.

A

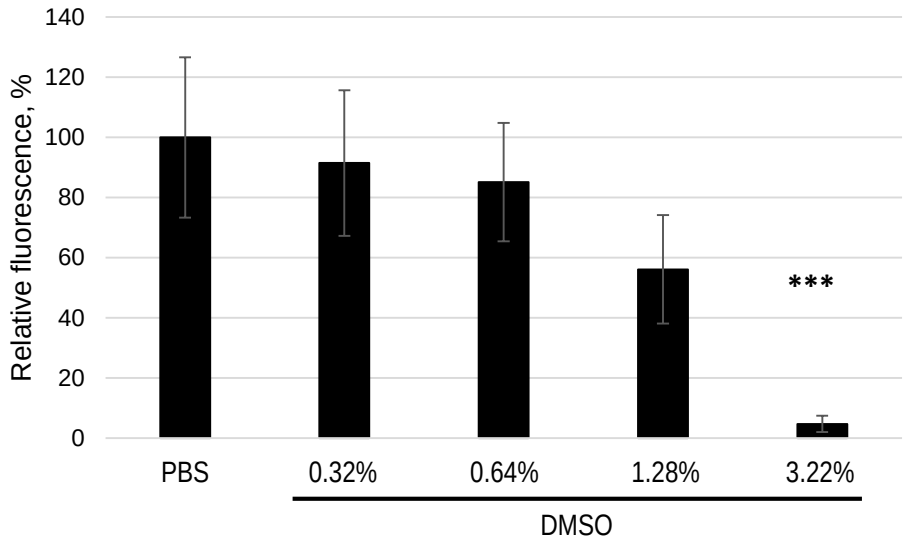
DMSO toxicity towards hFOB
Relative fluorescence, %
140
120
100
80
60
40
20
0
***
PBS
0.32%
0.64%
1.28%
3.22%
DMSO

B

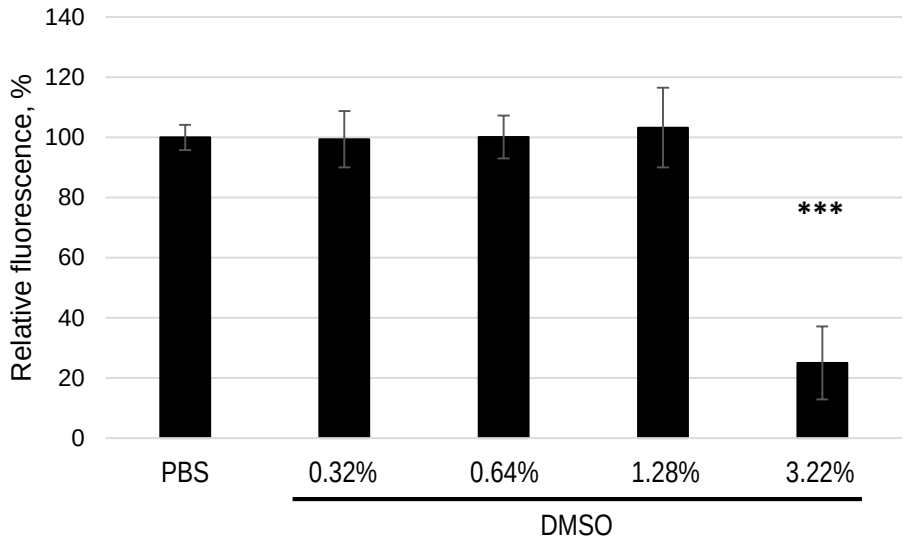
DMSO toxicity towards HUVEC
Relative fluorescence, %
140
120
100
80
60
40
20
0
***
PBS
0.32%
0.64%
1.28%
3.22%
DMSO

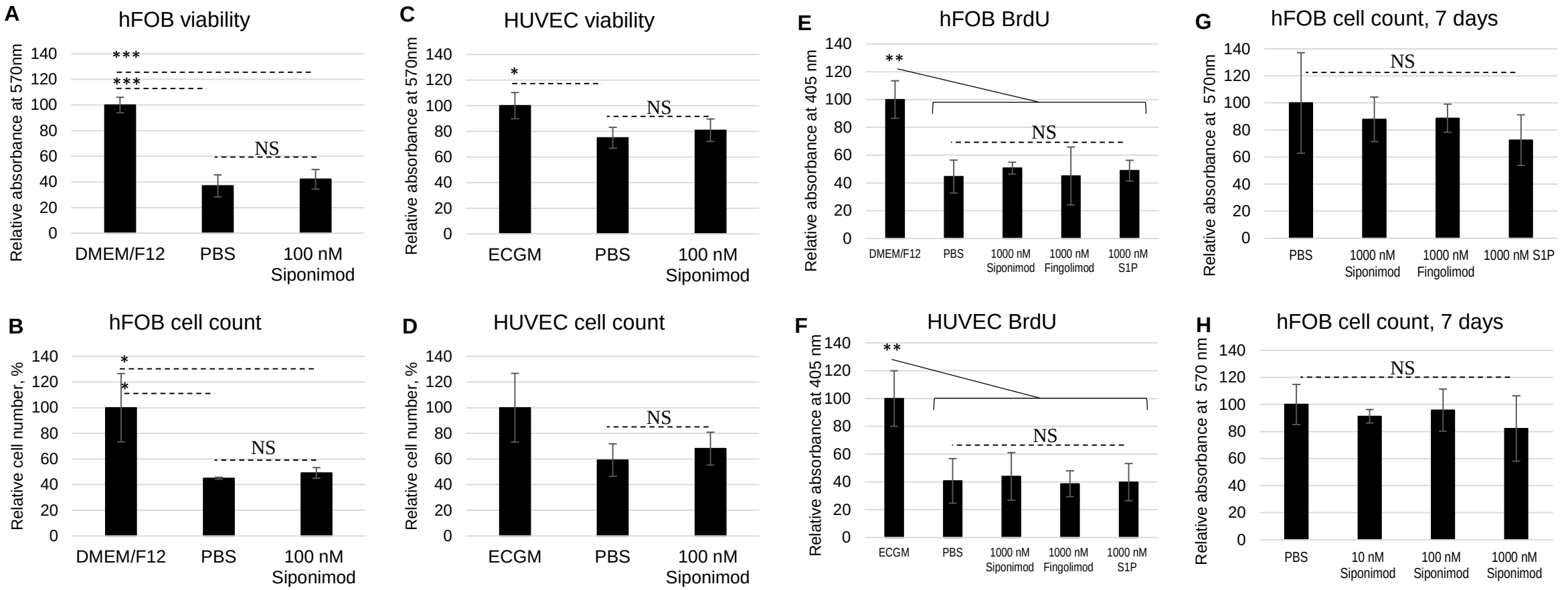
A
hFOB viability
Relative absorbance at 570nm
140
120
100
80
60
40
20
0
***
***
NS
DMEM/F12
PBS
100 nM Siponimod
C
HUVEC viability
Relative absorbance at 570nm
*
NS
ECGM
PBS
100 nM Siponimod
E
hFOB BrdU
Relative absorbance at 405 nm
**
NS
DMEM/F12
PBS
1000 nM Siponimod
1000 nM Fingolimod
1000 nM S1P
G
hFOB cell count, 7 days
Relative absorbance at 570nm
NS
PBS
1000 nM Siponimod
1000 nM Fingolimod
1000 nM S1P
B
hFOB cell count
Relative cell number, %
*
*
NS
DMEM/F12
PBS
100 nM Siponimod
D
HUVEC cell count
Relative cell number, %
NS
ECGM
PBS
100 nM Siponimod
F
HUVEC BrdU
Relative absorbance at 405 nm
**
NS
ECGM
PBS
1000 nM Siponimod
1000 nM Fingolimod
1000 nM S1P
H
hFOB cell count, 7 days
Relative absorbance at 570 nm
NS
PBS
10 nM Siponimod
100 nM Siponimod
1000 nM Siponimod

A

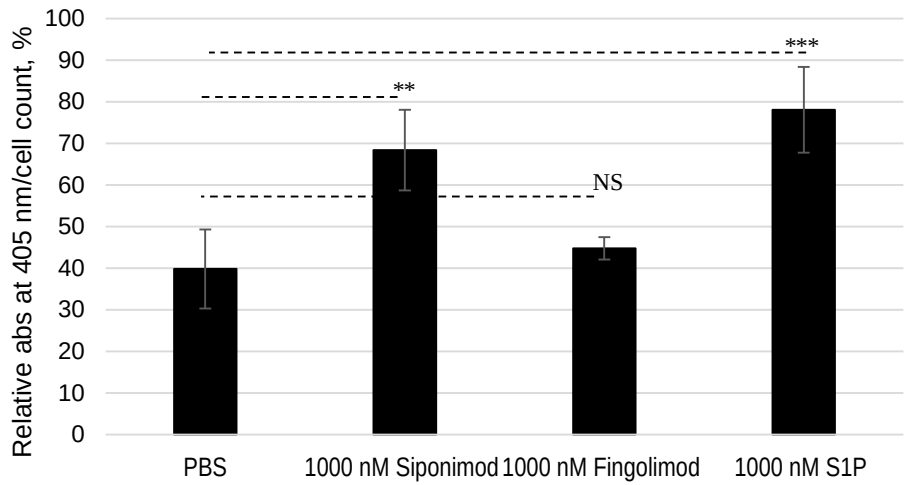
hFOB pNPP/count
Relative abs at 405 nm/cell count, %
100
90
80
70
60
50
40
30
20
10
0
**
***
NS
PBS
1000 nM Siponimod
1000 nM Fingolimod
1000 nM S1P

B

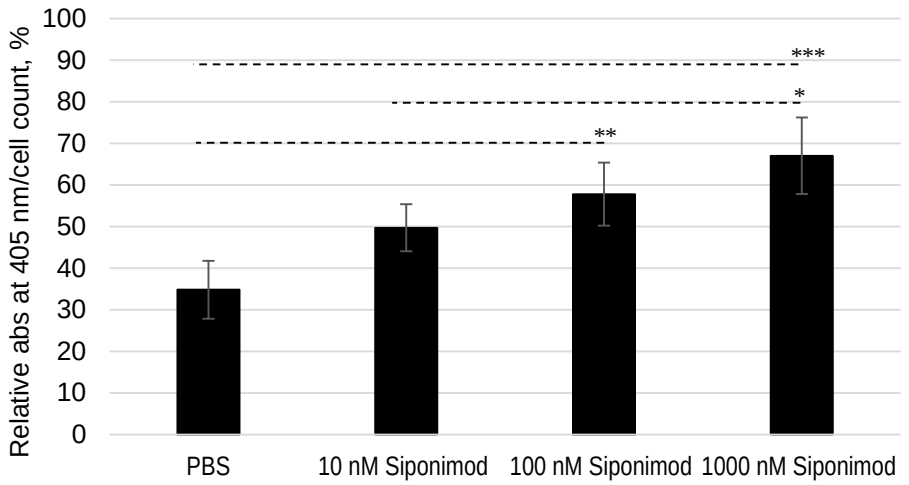
hFOB pNPP/count
Relative abs at 405 nm/cell count, %
100
90
80
70
60
50
40
30
20
10
0
**
*
***
PBS
10 nM Siponimod
100 nM Siponimod
1000 nM Siponimod

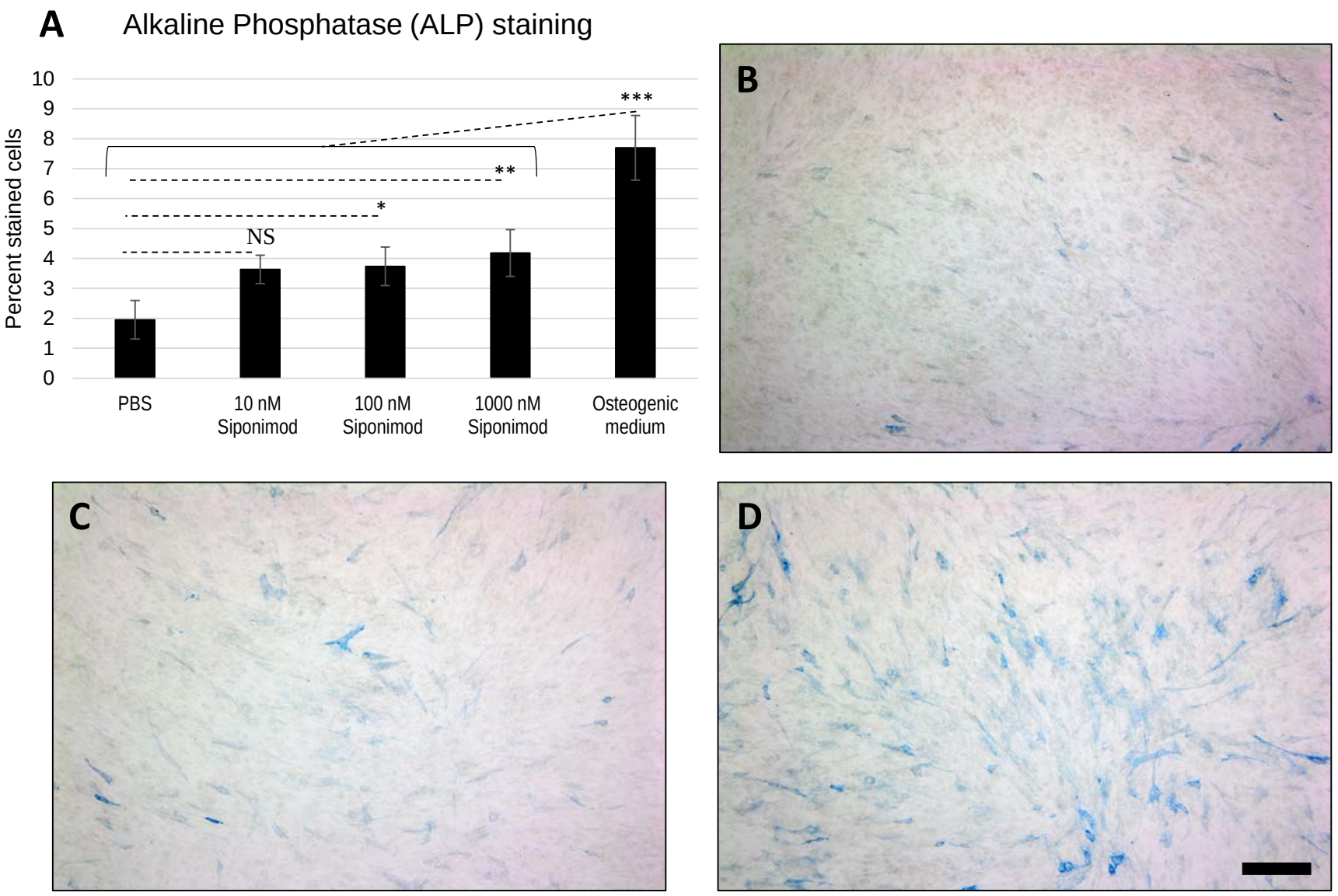
A
Alkaline Phosphatase (ALP) staining
Percent stained cells
10
9
8
7
6
5
4
3
2
1
0
***
**
*
NS
PBS
10 nM Siponimod
100 nM Siponimod
1000 nM Siponimod
Osteogenic medium
B
C
D

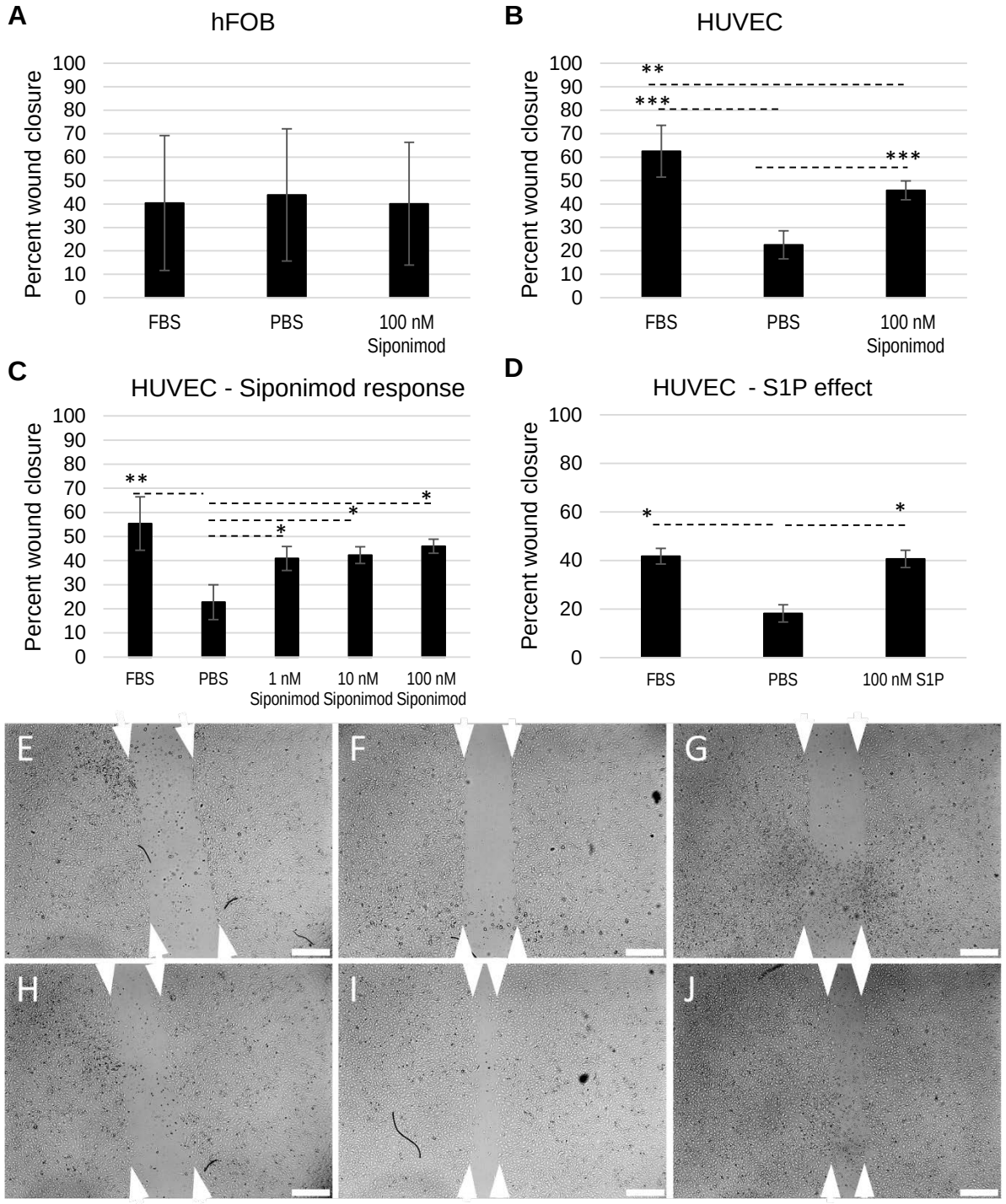
A
hFOB
Percent wound closure
100
90
80
70
60
50
40
30
20
10
0
FBS
PBS
100 nM Siponimod
B
HUVEC
**
***
***
Percent wound closure
FBS
PBS
100 nM Siponimod
C
HUVEC - Siponimod response
**
*
*
*
Percent wound closure
FBS
PBS
1 nM Siponimod
10 nM Siponimod
100 nM Siponimod
D
HUVEC - S1P effect
*
*
Percent wound closure
80
60
40
20
FBS
PBS
100 nM S1P
E
F
G
H
I
J

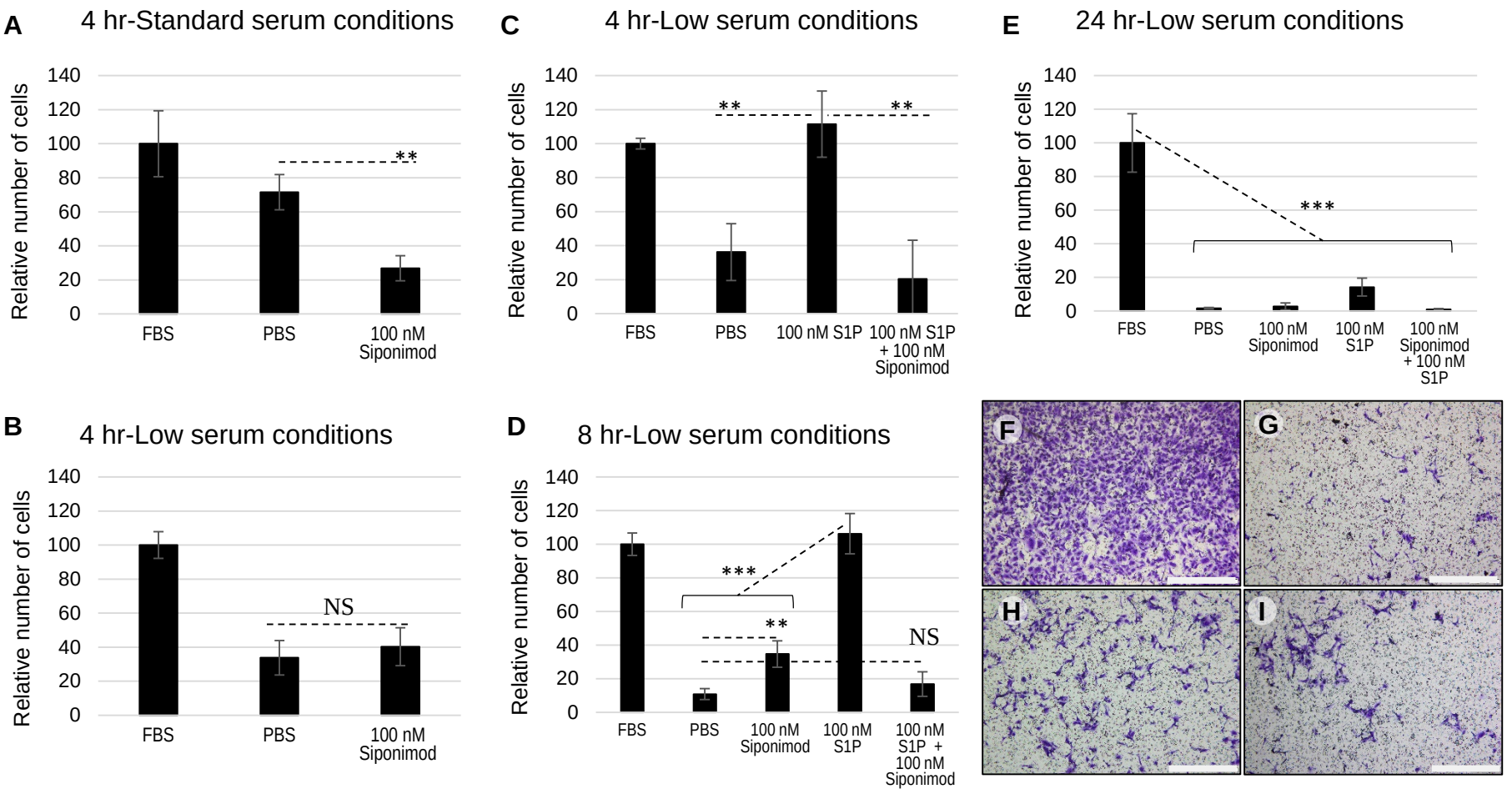
A
4 hr-Standard serum conditions
Relative number of cells
140
120
100
80
60
40
20
0
**
FBS
PBS
100 nM Siponimod
B
4 hr-Low serum conditions
Relative number of cells
NS
FBS
PBS
100 nM Siponimod
C
4 hr-Low serum conditions
Relative number of cells
**
**
FBS
PBS
100 nM S1P
100 nM S1P + 100 nM Siponimod
D
8 hr-Low serum conditions
Relative number of cells
***
**
NS
FBS
PBS
100 nM Siponimod
100 nM S1P
100 nM S1P + 100 nM Siponimod
E
24 hr-Low serum conditions
Relative number of cells
***
FBS
PBS
100 nM Siponimod
100 nM S1P
100 nM Siponimod + 100 nM S1P
F
G
H
I

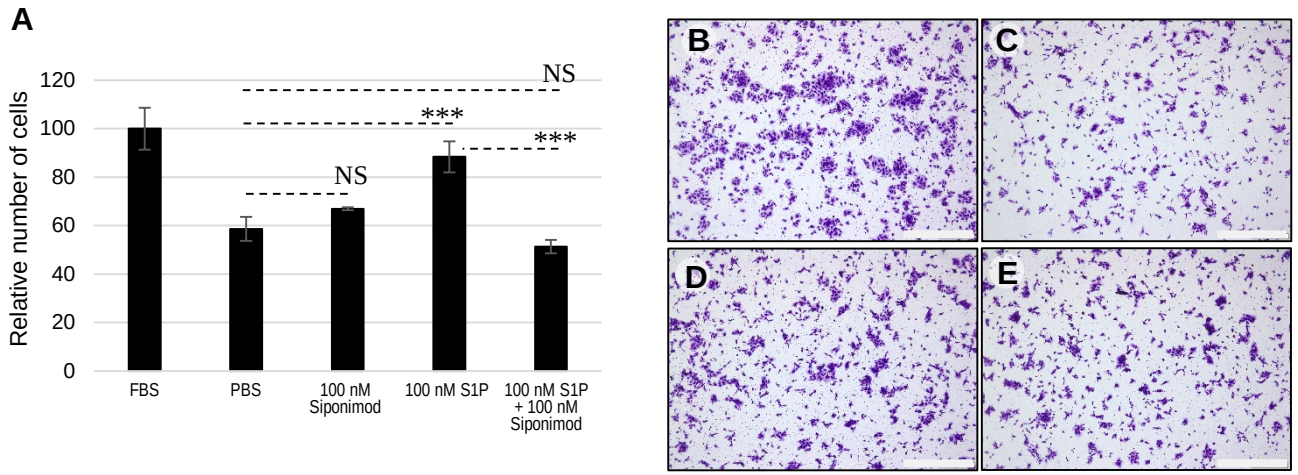
A
Relative number of cells
120
100
80
60
40
20
0
NS
***
***
NS
FBS
PBS
100 nM Siponimod
100 nM S1P
100 nM S1P + 100 nM Siponimod
B
C
D
E

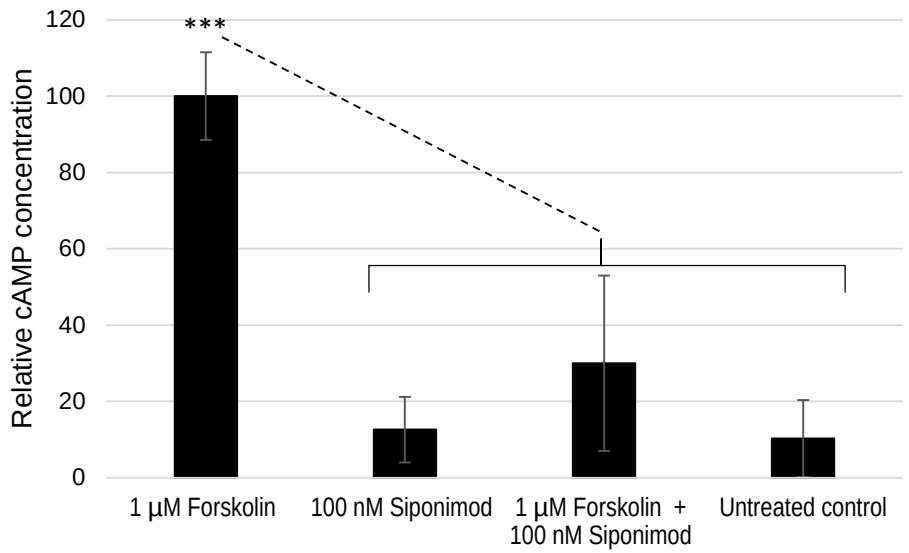
120
100
80
60
40
20
0
Relative cAMP concentration
***
1 µM Forskolin
100 nM Siponimod
1 µM Forskolin + 100 nM Siponimod
Untreated control